M. Shandor, A. R. Stone, and R. E. Walker

Secondary Gas Thrust

One of the foremost problems associated with solid-propellant rocket-propelled vehicles is attitude control. This is especially true of the larger vehicles, which accelerate slowly and maneuver at very high altitudes and for which the usually efficient aerodynamic surfaces are inadequate.

An obvious means of producing forces for controlling flight in these heavy vehicles is the deflection of rocket exhaust gases, or, as it is generally termed, thrust vector control (TVC). For liquid-propellant motors, TVC is achieved by gimballing the motor and nozzle. For the solid-propellant rocket, however, in which the nozzle and motor are constructed as a unit, this method is impossible. A way of overcoming this difficulty is to place in the supersonic exhaust flow an adjustable obstruction such as jet vanes like those used in the German V2 rockets, jet flaps or tabs, or jetevators (Fig. 1). But with such means, the heat resistance of available materials is a limiting factor. A more promising technique, which has been studied at APL, is the use of movable nozzles—a method analogous to gimballing the motor. Here again, however, heat resistance of the material, especially in the seals, is a serious problem.

Advances in solid-propellant technology, with consequent higher flame temperatures and large quantities of solid particles or liquid droplets in the exhaust flow, require TVC methods other than the aforementioned adjustable obstructions. Lateral injection of a fluid (liquid or gas) into the rocket exhaust is a method that, in principle, is ideally suited to the task. The practical application of this principle was demonstrated in 1952, when Hausman,[1] using air injected laterally into a supersonic airstream (both gases at ambient temperature), demonstrated the existence of a side force in addition to the usual jet reaction. Local high pressures associated with the induced shock wave produced by the injectant can yield a force equal to or greater than the jet reaction itself. This method provides thrust augmentation, albeit small, in contrast with other TVC methods.

Experimental Method

A research program has been under way at APL since early 1960, to study thrust vector control by secondary gas injection. A small hydrogen peroxide motor capable of about 100 lb of thrust at approximately a 1.0-lb/sec flow of catalytically decomposed 90% hydrogen peroxide provided a

[1] G. F. Hausman, *Thrust Axis Control of Supersonic Nozzles by Airjet Shock Interference*, United Aircraft Corporation, R-63143-24, May 1952.

Fluid-injection thrust vector control is rapidly being exploited for attitude control of solid-propellant ballistic missiles. This method of developing control forces removes moving parts completely from a hot-gas environment, leading to a more reliable control system. Interest at APL is centered on the physics of supersonic-flow/side-jet interaction.

Injection Vector Control

good starting point for the investigation. Experiments on temperature effects of injectant and propellant, nozzle geometry, point of injection, size of injectant orifice, and injectant species have been performed. This paper is limited to a study involving the effects of injectant-gas properties and injectant-orifice size in a conical rocket nozzle.[2]

[2] R. E. Walker, A. R. Stone, and M. Shandor, "Secondary Gas Injection in a Conical Rocket Nozzle," *J. Am. Inst. Aeronautics and Astronautics*, **I**, Feb. 1963, 334–338.

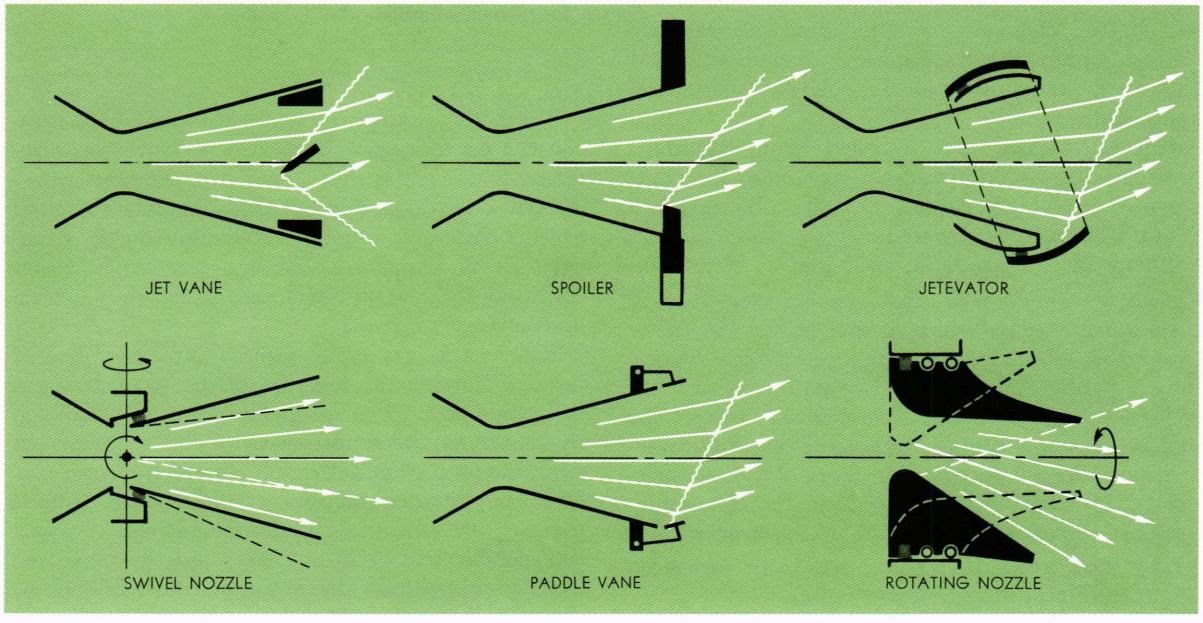

Fig. 1—Some mechanical thrust vector control schemes and associated flow deflection.

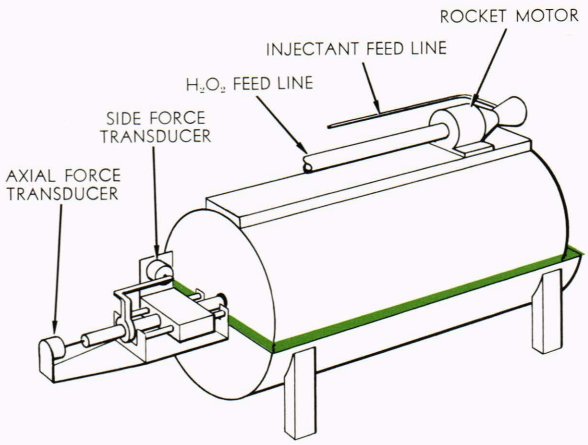

Fig. 2—General arrangement of the thrust stand, showing water flotation of the test equipment.

Motor operating conditions, nozzle geometry, and injectant location are fixed. Proposed future investigations will be concerned with secondary injection of both inert and reactive liquids.

The thrust stand consists of a rocket motor and nozzle mounted rigidly on the periphery of, and in line with, the axis of a water-floated drum (Fig. 2). The drum axle is mounted in anti-friction bearings that allow the drum to have simultaneous rotational and translational motion.

Force transducers are used to measure the axial thrust and turning moment developed by the nozzle. Propellant and injectant are fed to the test stand through relatively long rigid lines that introduce fixed spring constants superimposed on the elastic constants of the force transducers. Calibrations of the transducers, taken before and after tests, were shown to be independent of internal line pressures.

Injectant gases are supplied from standard compressed-gas containers. A maximum injectant pressure of 500 psia is used for carbon dioxide and about 1000 psia for the other gases. Injectant gas temperature is ambient, nominally 70°F. Injectant gas weight flow rate $\dot{W}_j$ is metered through a standard ASME* sharp-edged orifice flowmeter calibrated by timed discharge of carbon dioxide into a calibrated volume. Evaluation of the injectant-orifice discharge coefficient, using the metered gas flow rate and other measured parameters, provides a compatibility check of the measurements. It also serves as an indicator for sonic-subsonic injection transition. The liquid-propellant weight flow rate $\dot{W}$ is computed from measured quantities in isentropic flow relations.

* American Society of Mechanical Engineers.

TABLE I

PROPERTIES OF RESEARCH ROCKET MOTOR, NOZZLE, AND INJECTANTS USED IN SECONDARY GAS INJECTION EXPERIMENTS

Motor	
Propellant	90% H_2O_2
Exhaust gas composition	0.708 mole fraction H_2O 0.292 mole fraction O_2
Thrust coefficient	1.42
Pressure (P_o)	≈400 psi
Propellant flow rate ($\dot{W}$)	≈0.84 lb/sec
Exhaust gas total temperature (T_o)	1845°R
Specific heat ratio (γ)	1.266
Ambient pressure	Atmospheric
Injectant	
Gas	CO_2, N_2, He, He + Ar, Ar, and H_2
Injectant pressure (P_{oj})	40–1000 psi
Injectant total temperature (T_{oj})	≈70°F
Injectant port diameter (d_j)	0.0625, 0.089, 0.125, 0.180 in.
*Nozzle**	
Divergent half angle (α)	15°
Throat diameter (d_t)	0.501 in.
Exit diameter (d_3)	1.074 in.
Nozzle diameter at injectant port (d_1)	0.812 in.
Mach number at injection plane (M_1)	2.4
Exit Mach number (M_3)	2.8

* Conical, sharp-edged throat.

Temperature measurements are made with iron-constantan thermocouples, and pressure measurements with calibrated electrical pressure transducers. Where possible, all transducers are excited from a common, monitored voltage source. Temperature and pressure signals are recorded either continuously or with a six-point data sampler on a multichannel recorder.

Figure 3 is a sketch of the motor and conical nozzle, showing the location of the secondary gas injection port. The propellant gas is produced by catalytic decomposition of 90% hydrogen peroxide at a nominal motor chamber pressure of 400 psia. The decomposition products are 29 mole percent oxygen and 71 mole percent water vapor; the specific heat ratio is 1.266; and the measured average propellant exhaust temperature is 1845°R. Table I lists the conditions under which the test motor, nozzle, and injectants were operated.

Experimental Results

Two separate effects were studied, injectant orifice size and molecular weight of injectant, and in both sets of measurements the following conditions were held constant:

1. The axial position of the circular convergent injectant port was fixed and normal to the nozzle axis; and

2. Motor chamber pressure was kept at 400 psia.

The freestream Mach number at this point was 2.4. Static pressure of the undisturbed supersonic flow at the injection point P_1 was nominally 30 psia, and the exit Mach number of the nozzle was computed from the geometrical area ratio to be 2.8.

For studying the effects of orifice size, carbon dioxide at room temperature was selected as the injectant. Data were obtained for injectant orifice diameters of 0.0625, 0.089, 0.125, and 0.180 in., each nominally doubling the area of the previous port. The pressure ratio P_{oj}/P_1 across the injectant port was varied over a range sufficient to cover the cases of both subsonic and sonic flow through the orifices; the transition occurred at $P_{oj}/P_1 \approx 4$.

A summary of the data pertaining to orifice size is given in Fig. 4, in which the normalized specific impulse I_s/I_s^* is plotted as a function of the ratio of the weight flow of the injectant to that of the propellant $\dot{W}_j/\dot{W}$. The effective specific impulse I_s is obtained by dividing the force normal to the nozzle axis by the measured injectant weight flow rate. The force per unit weight flow (specific impulse) of a sonic jet of the injectant exhausting into a vacuum is I_s^*. The term I_s/I_s^* represents, therefore, an amplification factor for secondary injection. Because this factor is usually about two, fluid injection is rather efficient. Note in Fig. 4 that all sonic data correlate rather well. The most efficient performance is achieved in the vicinity of transition from sonic to subsonic injection for any one orifice. For a fixed pressure ratio across the orifice, small orifices are more efficient. The subsonic data appear to drop off to a limiting value of I_s/I_s^*.

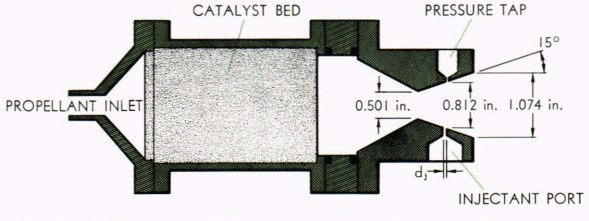

Fig. 3—Diagram of the rocket motor used in secondary gas injection experiments.

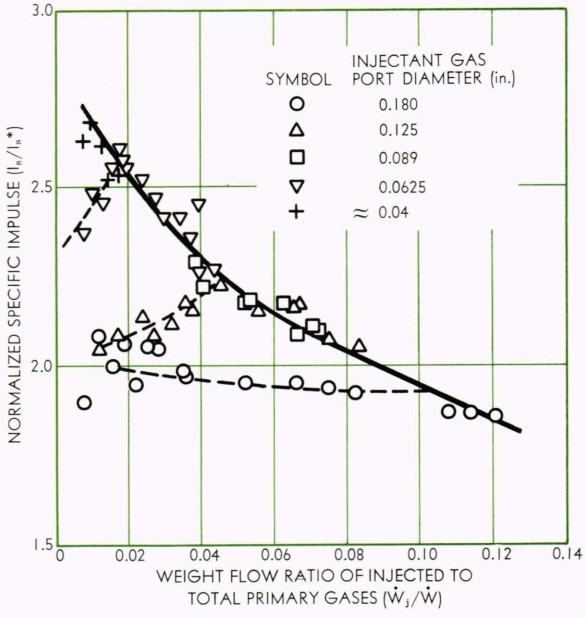

Fig. 4—Correlation of secondary gas injection data, with CO_2 injectant at 70°F. All subsonic injection data ($P_{oj}/P_1 < 4$) are flagged.

TABLE II

SOME PROPERTIES OF THE INJECTANTS USED IN SECONDARY GAS INJECTION STUDIES

Gas	*Molecular Weight* ($\mathfrak{M}_j$)	*Specific Heat Ratio* (γ_j)	*Sonic Specific Impulse* (I_s^*, *sec*)
CO_2	44.01	1.30	45.3
Ar	39.91	1.67	44.7
N_2	28.02	1.40	54.9
80 mole % He + 20 mole % Ar	11.18	1.67	84.4
He	4.00	1.67	141.2
H_2	2.02	1.40	204.8

The effects of molecular weight and specific heat ratio on secondary injection were investigated, using the gases listed in Table II. All of the injectants are inert, with the exception of H_2 which, in principle, could react with the hot O_2-H_2O exhaust products; no evidence of combustion was noted, however. Failure to ignite may be attributable to an exhaust temperature that is inadequate to support supersonic combustion at the prevailing pressures and residence times (about 10^{-5} sec). Ambient-temperature injection through a 0.0625-in.-diameter orifice was used throughout. Figure 5 is a plot of these data, with the experimental amplification factor normalized by dividing by a theoretical value.

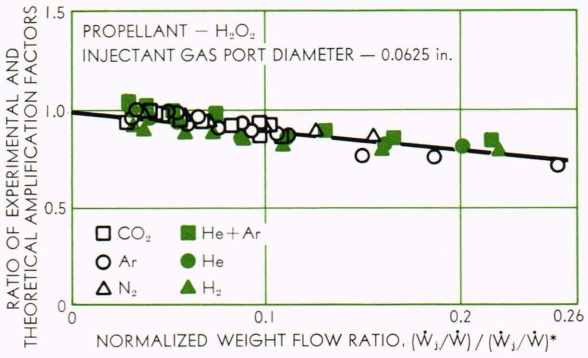

Fig. 5—Correlation of data from studies of the effects of molecular weight and specific heat ratio on secondary injection, using various injectant gases.

Analysis of Experimental Results

Results obtained in these experiments could not be correlated satisfactorily by any theory in the available literature. We have therefore constructed a simple model that gives results that are in qualitative agreement with the data. A somewhat simplified version of a detailed paper now in preparation on this analysis is presented here.

Consider the two-dimensional model shown in Fig. 6. To idealize the problem, assume constant-area mixing between a *trace* of injectant gas and a portion of the supersonic flow considered as an ideal gas. Injection is assumed to be normal to the supersonic stream, although the theory can be extended easily to other injection angles. Mixing is assumed to be instantaneous and dissipates the "normal" jet momentum. Injection causes a pressure rise and induces a weak shock wave in the surrounding supersonic flow. After constant-area mixing, the gases are assumed to expand isentropically until the static pressure equals that of the undisturbed supersonic flow. Pressure continuity is preserved along the dividing streamline. Small flow deflections are assumed so that linear supersonic theory will apply. The resulting transverse force is obtained by integrating the pressure along the dividing streamline. According to two-dimensional linear supersonic flow theory,[3] the pressure coefficient

$$\frac{\delta p}{p\gamma M^2/2} = \frac{2}{\sqrt{M^2-1}}\left(\frac{dy}{dx}\right)_{str}, \qquad (1)$$

where $(dy/dx)_{str}$ is the streamline slope, and M is Mach number. The side force ΔF becomes

$$\iint (\delta p)\, dxdz = \frac{\gamma M^2}{\sqrt{M^2-1}}\, p\Delta A. \qquad (2)$$

The $p\Delta A$ term is evaluated from generalized one-dimensional flow theory[4] and is proportional to the trace injectant flow rate $\dot{W}_j$. Dividing this force by the injectant flow rate, i.e. $\Delta F/\dot{W}_j$, we obtain the effective specific impulse I_s. For normal injection into a semi-infinite two-dimensional supersonic stream, assuming ideal inert gases, the amplification factor is derived:

$$\frac{I_s}{I_s^*} = \left\{\frac{\gamma_j}{1+\gamma_j}\cdot\frac{\gamma M^2}{M^2-1}\cdot\frac{1}{[2+(\gamma-1)M^2]}\right\}^{1/2} \times$$

$$\left\{\frac{[2+(\gamma-1)M^2][1+\mathfrak{M}_j/\mathfrak{M}+(C_{pj}/C_p)(T_{oj}/T_o-1)]}{2[(\mathfrak{M}_j/\mathfrak{M})\,(T_{oj}/T_o)]^{1/2}} - \frac{M^2(C_{pj}/C_p)\,(1-\gamma/\gamma_j)}{2[(\mathfrak{M}_j/\mathfrak{M})(T_{oj}/T_o)]^{1/2}}\right\}, \qquad (3)$$

where γ is specific heat ratio, T_o is stagnation temperature, $\mathfrak{M}$ is molecular weight, C_p is $\gamma\mathfrak{R}/(\gamma-1)$ —molar specific heat at constant pressure, and $\mathfrak{R}$ is universal gas constant. Where subscripts are lacking, freestream conditions are referred to, and j subscripts refer to the injectant. Values of theoretical I_s/I_s^* for the various gases are given in Table III. Equation (2) can be modified for injection angles other than 90°, such as one might anticipate for our subsonic injection.

Equation (3) is valid for trace injectant rate only, i.e. $\dot{W}_j \ll \dot{W}$. As such, it neglects mixing and shock losses and is not entirely realistic. If the mixing proportions are finite, the mathematics of Eq. (3), though involved, are straightforward; I_s/I_s^* is then a function of the mixing proportions. However, there is a maximum rate at which a foreign gas can be added to a constant-area supersonic flow. At this maximum, the supersonic stream "chokes"—is decelerated to $M = 1$, a

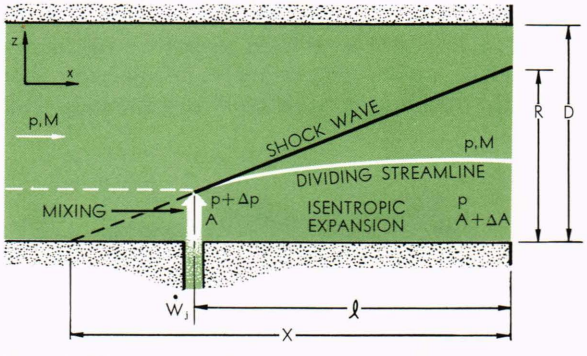

Fig. 6—"Linearized" model for fluid-injection analysis.

[3] A. H. Shapiro, *The Dynamics and Thermodynamics of Compressible Fluid Flow*, Ronald Press Co., New York, 1954, Chap. 14.

[4] Shapiro, *op. cit.*, Chap. 8.

TABLE III

THEORETICAL VALUES OF I_s/I_s^* AND $(\dot{W}_j/\dot{W})^*$‡ (H_2O_2 PROPELLANT)

Gas	I_s/I_s^*	$(\dot{W}_j/\dot{W})^*$
CO_2	2.65	0.392
Ar	2.88	0.344
N_2	2.41	0.336
80 mole % He + 20 mole % Ar	2.32	0.219
He	2.57	0.123
H_2	2.56	0.090

‡ Respectively, the amplification factor and the ratio of jet flow to primary flow causing choking.

condition we can regard as limiting. The value of I_s/I_s^*, based upon a "choked" model, can be as low as 70% of the values obtained from Eq. (3) for our experimental condition. This is a nonlinear effect.

From Fig. 5 we see that performance drops off with increasing sonic injection rate. This attenuation can be attributed to nonlinear effects, to reflections of the induced shock wave from the nozzle wall, and to incomplete expansion of the mixed gases before exhaust.

Within the restrictions of linear theory, attenuation due to reflected shock waves is a function of R/D, where R is the radius of the induced shock wave at the nozzle exit and D is the nozzle exit diameter. For a Mach cone, $R = X/\sqrt{M^2 - 1} = h + l/\sqrt{M^2 - 1}$, where l is the distance between the orifice and nozzle exit and h is the radius of the semicircular mixing plane or depth of penetration. If we assume "choked" flow (maximum mixing), it can be shown that

$$\frac{h}{D} \approx \sqrt{\frac{(\dot{W}_j/\dot{W})}{2(\dot{W}_j/\dot{W})^*}}, \qquad (4)$$

and

$$\frac{R}{D} \approx \frac{l}{D\sqrt{M^2 - 1}} + \sqrt{\frac{(\dot{W}_j/\dot{W})}{2(\dot{W}_j/\dot{W})^*}}, \qquad (5)$$

where $\dot{W}_j/\dot{W}$ is the weight flow ratio of injected gases to total primary gases, and $(\dot{W}_j/\dot{W})^*$ is the ratio giving "choked" flow which depends only on primary and secondary gas properties (γ, T, $\mathfrak{M}$) and Mach number. Values of $(\dot{W}_j/\dot{W})^*$ are given in Table III. Equation (5) assumes $h \ll D$. When $R/D = 1$, the shock wave touches the opposite wall and a transverse force approaching zero (or even negative) can be expected. If the shock wave is completely reflected ($R/D > 1$), the system behaves as though the perturbation emanated from the opposite wall.

Incomplete expansion of the mixed gases implies small l values for any given D value. All of the available pressure rise due to mixing is not impressed on the nozzle wall. For undisturbed supersonic flow, a midstream perturbation that is a distance h from the wall only influences wall pressures at distances greater than $h\sqrt{M^2 - 1}$ downstream. Therefore, for injection near the nozzle exit, one might speculate that performance will depend upon the dimensionless ratio $h\sqrt{M^2 - 1}/l$. Assuming "choked" mixing,

$$\frac{h\sqrt{M^2 - 1}}{l} = \left(\frac{D\sqrt{M^2 - 1}}{l}\right)\sqrt{\frac{(\dot{W}_j/\dot{W})}{2(\dot{W}_j/\dot{W})^*}}. \qquad (6)$$

In Fig. 5, which is the plot of data on injectant species, $l/D\sqrt{M^2 - 1}$ is a constant since the point of injection was fixed. Therefore, both attenuation due to reflected shock waves and incomplete expansion of mixed gases are handled by the independent variable $(\dot{W}_j/\dot{W})/(\dot{W}_j/\dot{W})^*$. Note that the data, with the exception of He, lie well within ±10% of the average curve. The low He values were not accounted for.

Supplemental Investigations

For further studies we decided to eliminate problems associated with the conical nozzle, e.g. variation of Mach number and shock waves inherent in conical nozzles. Two axially symmetric sharp-corner-throat contoured nozzles (exit diameter = 1.0 in.) were fabricated, one giving $M = 1.86$, and the other $M = 2.90$, with decomposed hydrogen peroxide. Shadowgraphs showed both to be essentially free of shock waves. The nozzles are so designed that constant-area ducts can be rigidly clamped to the exit to provide a constant-Mach-number test region. This system proved to be very flexible for a variety of tests. A repetition of the experiments, in which injectant orifice size was changed and where the propellant gases were either H_2O_2 or ambient air, supported the conical-nozzle results. The data were quite satisfactorily handled by our analytical model. In addition, we conducted studies in which the length of the tailpipe downstream from the injection point was varied. The effects of reflected shock waves and incomplete expansion were evident as predicted. Data have also been obtained for multiple orifice injection, varying motor pressure, and inert hot-gas injection (preburned air or O_2 + trace H_2).†

† To be published.